Spectrochimica Acta Part A: Molecular and Biomolecular Spectroscopy 133 (2014) 591–596

Contents lists available at ScienceDirect

Spectrochimica Acta Part A: Molecular and Biomolecular Spectroscopy

journal homepage: www.elsevier.com/locate/saa

Surface enhanced Raman scattering study of the antioxidant alkaloid boldine using prismatic silver nanoparticles

M.A. Herrera, G.P. Jara, R. Villarroel, A.E. Aliaga, J.S. Gómez-Jeria, E. Clavijo, C. Garrido, T. Aguayo, M.M. Campos Vallette *

Universidad de Chile, Faculty of Sciences, PO Box 653, Santiago, Chile

HIGHLIGHTS

- The SERS spectrum of the antioxidant alkaloid boldine has been registered.
- Spectral SERS reproducibility is obtained by using of prismatic silver nanoparticles.
- Theoretical calculations predict the orientation of boldine onto the Ag surface.

GRAPHICAL ABSTRACT

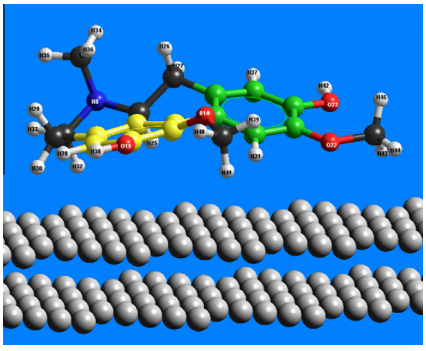

ARTICLE INFO

Article history:
Received 30 August 2013
Received in revised form 26 May 2014
Accepted 27 May 2014
Available online 14 June 2014

Keywords:
Prismatic silver nanoparticles
Boldine
Surface enhanced Raman scattering
Extended Hückel Theory

ABSTRACT

Prismatic silver nanoparticles (PNps) were used in the surface enhanced Raman scattering (SERS) study of the antioxidant alkaloid boldine (5,6,6a,7-tetrahydro-1,10-dimethoxy-6-methyl-4H-dibenzo[de,g]quinoline-2,9-diol). Prismatic and quasi-spherical (QsNps) silver nanoparticles were synthesized and characterized by UV–Vis spectra, topographic profile (AFM) and zeta potential measurements. Raman and infrared (IR) spectra of the boldine were registered. Theoretical model calculations of the boldine onto the Ag surface predict a nearly coplanar orientation of the benzo[de]quinoline moiety and non-bonded interactions (electrostatic).

Introduction

The boldo (*Peumus boldus*) is an endemic tree from Chile. The boldo leaves extract is of great interest to pharmaceutical industry, as it possesses high antioxidant activity due to its content of flavonoids and alkaloids. Boldine (5,6,6a,7-tetrahydro-1,10-dimethoxy-6-methyl-4H-dibenzo[de,g]quinoline-2,9-diol) is an aporphine alkaloid, associated with biological activities such as anti-tumor promoting, anti-inflammatory and antipyretic [1]. Boldine protect fish oil against thermal peroxidation displaying an activity similar to that of the quercetin flavonoid [2].

Different alkaloids have been studied by Raman and IR techniques, and computational calculation methods. Baranska et al. [3] studied the tobacco alkaloids (nicotine, nornicotine, cotinine, anabasine) using Raman spectroscopy and supported by Density Functional Theory (DFT) calculations at the B3LYP/aug-cc-pVDZ level of theory; for all tobacco alkaloids the characteristic Raman bands were assigned. A vibrational analysis was performed on the molecular structure of boldine hydrochloride using QM/MM

* Corresponding author. Tel.: +56 229787261.
E-mail address: facien05@uchile.cl (M.M. Campos Vallette).

http://dx.doi.org/10.1016/j.saa.2014.05.070
1386-1425/

[4]; geometry, harmonic vibrational frequencies and IR intensities were calculated by QM/MM method with B3LYP/6-31G(d) and universal force field (UFF) combination using the ONIOM code. Srivastava et al. [5] studied by IR, Raman and quantum chemistry the structural and spectral characteristics of boldine; electrostatic potential surface, optimized geometry, harmonic vibrational frequencies, IR intensities and activities of the Raman scattering were calculated by *ab initio* Hartree–Fock (HF) and DFT, employing B3LYP with a complete relaxation in the potential energy surface using the 6-311G(d,p) basis set.

The Raman spectral signal intensity is dramatically enhanced from a determined analyte–metal nanoparticle interaction, giving rise to the surface-enhanced Raman scattering (SERS); this technique has been applied to the detection of drugs, pesticides, explosives, and in the identification of nanostructures, biosensors, tumors and cancer cells. Cañamares et al. [6] studied the protoberberine alkaloids (palmatine, jatrorrhizine, and coptisine) by using SERS in combination with DFT calculations. The SERS of boldine has not been reported, probably due to the antioxidant properties which could induce high reactivity with the metal nanoparticles, avoiding obtaining a reproducible SERS spectrum. A SERS study of quercetin and related flavonoids was reported [7], showing chemical changes in the quercetin structure. Jurasekova et al. [8] demonstrate that the interaction of the quercetin with silver nanoparticles (prepared by reduction with citrate) and metal ions (Cu(II), Zn(II), Ag(I)) produces the formation of chelates as a result of the oxidation of the flavonoid, involving successive polymerization.

The aim of the present contribution deals with the preparation and characterization of prismatic (PNps) and quasi-spherical Ag nanoparticles (QsNps) for the SERS study of boldine (prepared by reduction with borohydride). The SERS of boldine has not been reported, probably due to the antioxidant properties which could induce high reactivity with the metal nanoparticles, avoiding obtaining a reproducible SERS spectrum. The spectral assignment of the SERS data is supported on our own Raman data; the analyte metal surface interaction nature is analyzed from the SERS band analysis of the hydroxyl group and the theoretical calculations of a molecular model for the boldine interacting with the Ag surface.

Experimental

Samples

Solid boldine, with a purity of 99.2% was used without further purification. The structure of boldine is shown in Fig. 1. The following chemicals were used for the preparation of the nanoparticle colloidal solutions: tri-sodium citrate dihydrate (99%, Merck), silver nitrate 99.9999% metal basis (Aldrich), hydrogen peroxide 30% (Merck), potassium bromide (FT-IR grade >99%, J.T. Baker Chemicals), and sodium borohydride (Merck GR for analysis). All chemicals were used as received.

Colloids preparation

Silver prism colloids were prepared following Frank et al. [9]. Some modifications to the reference procedure were performed, in particular, the time prior to the addition of the reducing agent standard solutions were prepared using ultrapure water 0.055 μS/cm conductivity: 1.25×10^{-2} M tri-sodium citrate, 3.75×10^{-4} M silver nitrate, 5.0×10^{-2} M hydrogen peroxide, 1.0×10^{-3} M potassium bromide and 5.0×10^{-3} M sodium borohydride (reducing agent). To six 20 mL Pyrex test tubes, the following reagents were added in the order: 2.0 mL of 1.25×10^{-2} M sodium citrate, 5.0 mL of 3.75×10^{-4} M silver nitrate, and 5.0 mL of 5.0×10^{-2} M H_2O_2. Then,

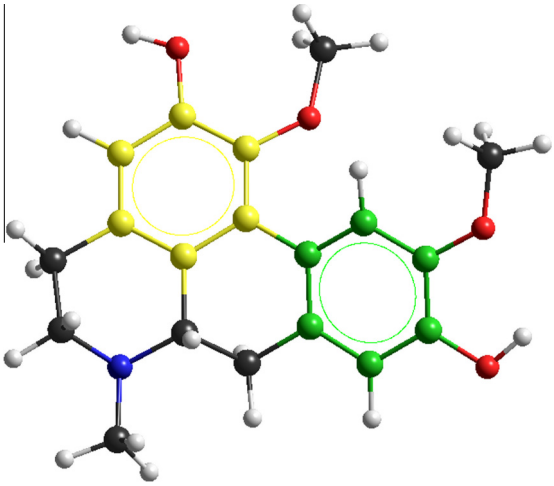

Fig. 1. The structure of boldine. The benzo[de] and benzo[g] quinolinic rings are represented by yellow and green colors, respectively. (For interpretation of the references to color in this figure legend, the reader is referred to the web version of this article.)

to each vial a different volume of 1.0×10^{-3} M KBr was added as follows: 0, 10, 15, 20, 25 and 40 μL. To start the synthesis step, 2.5 mL of freshly prepared 5.0×10^{-3} M sodium borohydride were added within no more than 10 min after preparation. Then, the solution was abruptly and totally added to each vial under simultaneous stirring. Once all reagents were combined, the caps were placed on the vials and they were carefully swirled using a Vortex mixer during about 2 min. The progression of the reaction becomes evident through the visual changes consistent with the morphological modification from the quasi-spherical to prismatic and growing of the silver nanoparticles. Typically, the sequence of color changes from yellow to orange to red to purple to violet to blue to pale greenish blue for the largest nanoprisms. It takes approximately 3 min to reach a stable color. The size and shape of the nanoparticles are controlled by the KBr addition which induces halt of the process. Fig. 2 displays the colloidal solutions from blue (0 μL) to yellow (40 μL) obtained by increasing the KBr concentration. In order to increase the PNps nanoparticles concentration, 1.5 mL of the PNps colloidal solutions were centrifugated at 10,000 rpm during 30 min; 1 mL of the supernatant was extracted. 0.5 mL of the solution was used for the SERS experiments.

Colloids characterization

UV–Vis–NIR extinction spectra of the six colloidal solutions display maxima at 714, 681, 681, 502, 495 and 424 nm, see Fig. 3. The

Fig. 2. Colloidal solutions from yellow to blue obtained by dilution of the KBr solution (2.75×10^{-6}, 1.72×10^{-6}, 1.38×10^{-6}, 1.03×10^{-6}, 6.90×10^{-7}, 0.0 M). (For interpretation of the references to color in this figure legend, the reader is referred to the web version of this article.)

size distribution of the nanoparticles is in the range 20–50 nm, with the most probable size around 30 nm [9]. A control of the purity of the colloidal solution was carried out by measuring the Raman spectrum from aggregates dried over a quartz slide at room temperature. AFM data indicate that the yellow colloid is composed by quasi-spherical nanoparticles in the 20–35 nm range. The blue colloids contain nanoprisms having a thickness near 7 nm.

Instrumentation

All UV–Vis–NIR extinction spectra were recorded at room temperature on a double-beam spectrophotometer Shimadzu model UV-1800 in the 200–1100 nm spectral range and using a quartz cuvette with a 10 mm optical path.

AFM morphology data were obtained at room temperature with a NTegra Prima system operating in semicontact mode using single crystal silicon tips of 300 kHz. Nanoparticle samples are deposited on mica by using the spin-coating technique at 2000 rpm during 1 min. Synthesis residues were eliminated from several deionized water dilutions followed by centrifugation; the last process increases the Nps concentration. Thus, the topographic characterization is performed.

The hydrodynamic size distribution, viscosity and zeta potential measurements of QsNps and PNps were performed using Zetasizer NanoZS (Malvern) at 25 °C. The Nano ZS contains a 4 mW He–Ne laser operating at a wavelength of 633 nm and an avalanche photodiode detector. The scattered light was detected at an angle of 173°. Data were collected three times for each solution in 1 mL flux cells. The zeta potential is estimated from the Nps electrophoretic mobility by using the Smoluchowski approximation.

The IR data of boldine in KBr pellets were obtained from a FT-IR-Raman Perkin–Elmer series 2000 apparatus equipped with a DTGS detector and using a 4 cm^{-1} spectral resolution. The Raman and SERS spectra of boldine were measured with a Renishaw micro-Raman system (RM1000) using as excitation the 785 nm laser line. This instrument is equipped with a Leica DM/LM microscope, and an electrically cooled CCD camera. The signal was calibrated by using the 520 cm^{-1} line of a Si wafer and a 50× objective. The laser power on the sample was 2 mW. The resolution was set to 4 cm^{-1} and 5–20 scans of 10 s each were averaged. Spectra were recorded in the 200–1800 cm^{-1} region by using the 50× objective.

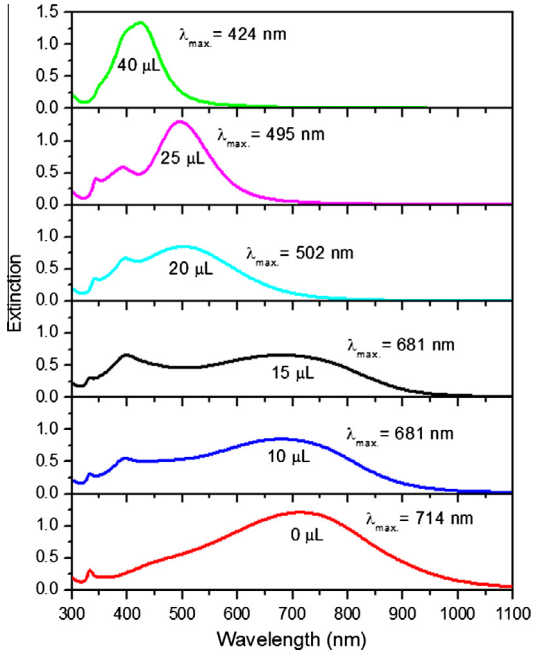

Fig. 3. UV–Vis–NIR extinction spectra of silver nanoprisms obtained by adding 0–40 µL of a KBr 10^{-3} M solution.

Sample preparation for Raman and SERS measurements

The Raman spectra of solid boldine were registered on a quartz slide. The extracted boldine powders were mixed with the silver colloidal solution up to a final concentration of 10^{-3} mol/L. The boldine sample was left in a closed chamber to interact with the silver colloid; the solution at pH near 7 was let settle for at least 12 h. This pH corresponds to the protonated boldine [10]. The SERS spectrum of boldine was obtained in colloidal solution (10^{-3} M); 85 µL of the colloidal solution was then placed onto a PCR tube cap. The SERS spectrum of boldine was obtained from a dried colloid (10^{-4} M of boldine); 10 µL are extracted from the 10^{-4} M solution and deposited onto a quartz slide and dried at room temperature.

Molecular models and calculations

The silver surface was simulated by building a big Ag cube with a face centered-cubic structure (a = 0.408 nm) as in our previous studies [11–14]. The resulting structure was trimmed to get a double Ag planar layer composed by 324 atoms. Molecular mechanics (MM-OPLS) was employed to optimize the boldine–Ag surface system keeping constant the metallic layer geometry. Extended Hückel Theory (EHT) was used to calculate the wave function of boldine as an isolated system and interacting with the metal surface. Hyperchem program was used [15]. EHT calculations produce qualitative or semiquantitative descriptions of molecular orbital and electronic properties [16] thus, describing the possible formation of double bonds. The combination of EHT with molecular mechanics provided qualitative explanations of our previous SERS results in peptides [14,17,18], nanotubes [11], tryptophan [12], lysine [13], humic acids [19] and 4-hydroxyproline and proline [20] interacting with Ag surfaces. EHT was chosen because it was shown that, within the Hartree–Fock–Rüdenberg picture, it is compatible with the nonempirical Hartree–Fock method in Roothaan's form [21,22]. IR and Raman spectra (not shown here) were calculated after full geometry optimization at the B3LYP/6-31G(d,p) level of the theory with the Gaussian package of programs [23].

Results and discussion

The shape, size and aggregation of the metal colloids solutions change the extinction spectrum (field profile and intensity) [24]. Figs. 3 and 4 show the extinction spectra of quasi-spherical (λ_{max} 424 nm) to prismatic (λ_{max} 714 nm) silver nanoparticles by modifying the KBr concentration. UV–Vis–NIR extinction spectra of the six colloidal solutions display maxima at 714, 681, 681, 502, 495 and 424 nm. The size distribution of the nanoparticles is in the range 20–50 nm, with the most probable size around 30 nm [9]. The observed color changes from yellow to blue by KBr concentration decreasing, Fig. 2, are associated to a silver nanoparticles morphology evolution in agreement with Lee et al. [25]; the variation of the morphologic characteristics (shape or size) is inferred from the SPR spectrum and SEM data. Thus, the present yellow and blue colloidal solutions contain quasi spherical (QsNps) and prismatic (PNps) nanoparticles, respectively; both were characterized by topographic profile (AFM) and zeta potential measurements.

The topographic profiles of PNps and QsNps obtained from AFM data indicate that these systems display height profile of 8 nm and

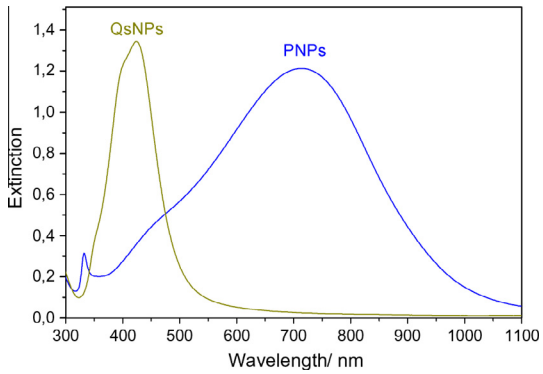

Fig. 4. UV–Vis spectra of quasi-spherical (QsNps) and prismatic (PNps) nanoparticles.

30 nm, respectively; this is in agreement with previous analysis [9]. Fig. 5 shows the topographic images and the height profile of the prisms and quasi-spheres. They were selected for the SERS study.

The hydrodynamic size distribution, viscosity and zeta potential measurements of PNps and QsNps colloidal solution were measured. The most probable diameter of PNps is 34.5 nm, the viscosity and zeta potential are 0.8872 cP and −49.0 mV, respectively. In the case of the QsNps the most probable diameter is 96.2 nm, the viscosity and zeta potential are 0.8872 cP and −48.4 mV, respectively. Since the zeta potential for both kinds of nanoparticles are similar it is expected that it aggregation should not be different; on the other hand the size of both nanoparticles is different. Thus, the SERS activity of both surfaces should be rather related to the morphology than to the surface charge. In the case of the colloids prepared by reduction with hydroxylamine (spherical nanoparticles), the zeta potential and the size are similar to those of the QsNps here reported.

The IR and Raman spectra of boldine in Fig. 6, are highly consistent with what is expected for a C_1 symmetry group, that is identical Raman and IR activity. The following band assignment is based on published data by Misra et al. [4], Srivastava et al. [5] and characteristic group frequencies [26,27]. Aromatic VCC vibrations are observed in IR at 1498, 1519, 1580 and 1600 cm^{-1} and in Raman at 1525 cm^{-1} and around 1600 cm^{-1} (three bands). At least three IR bands from 1380 to 1470 cm^{-1} are ascribed to aliphatic CH deformation modes; the bands at 1384 and 1467 cm^{-1} are CH_3 deformation modes. Bands belonging to N–CH_3 stretching modes are observed in the range 1270–1420 cm^{-1}. Phenolic vibrations are ascribed to IR bands at about 1090 and 1210 cm^{-1} while the ether function (CH_3–O–Phe) is represented by IR bands at 1081, 1130, 1176 and 1240 cm^{-1}. A CO vibration is assigned to the band observed in IR at 1017 cm^{-1} (1021 cm^{-1} in Raman). The medium IR bands at 770, 814, 869, 892 and 983 cm^{-1} are assigned to out of plane CH modes. Two Phe–OH deformation modes are ascribed to the bands at 609 and 388 cm^{-1}, observed in the IR and Raman spectra, respectively. The IR band at 564 cm^{-1} is probably due to a deformation mode of the Phe–O–CH_3 moiety.

Boldine shows a low solubility in water. 10 μL of a 10^{-3} M solution of boldine and the QsNps and PNps colloidal solutions were deposited onto a quartz slide. A SERS spectrum of boldine obtained by using the nanoprism colloidal solution displays an important fluorescence contribution. The SERS signals were clearly observed by increasing the boldine concentration. On the other hand the same resulting solution is dried on a quartz slide. Under the microscope, at 50× magnification, it is possible to observe boldine crystals and colloidal aggregates with boldine, see Fig. 7. The SERS signals of boldine were obtained using the colloidal aggregates.

The SERS spectrum of boldine 10^{-3} M in colloidal solution (Fig. 8B) is scanned after 3 h settle. The spectral profile of the SERS

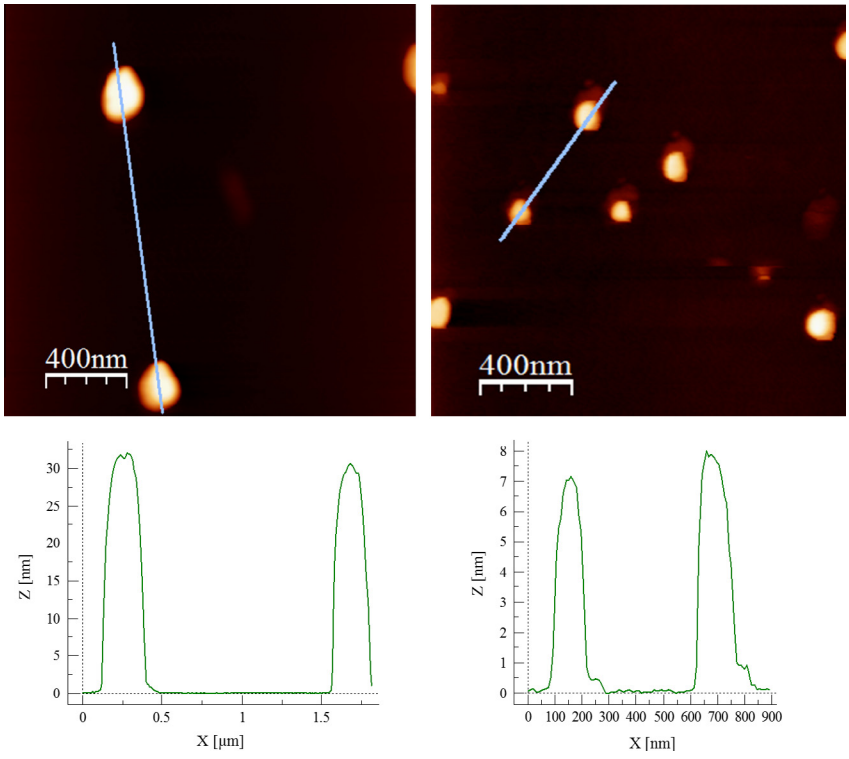

Fig. 5. Topographic images of prisms deposited on mica (A) yellow prisms, (B) blue prisms, (C) topographic profile of yellow prisms and (D) topographic profile of the blue prisms. AFM of QsNps (A) and PNps (B) deposited on mica. (For interpretation of the references to color in this figure legend, the reader is referred to the web version of this article.)

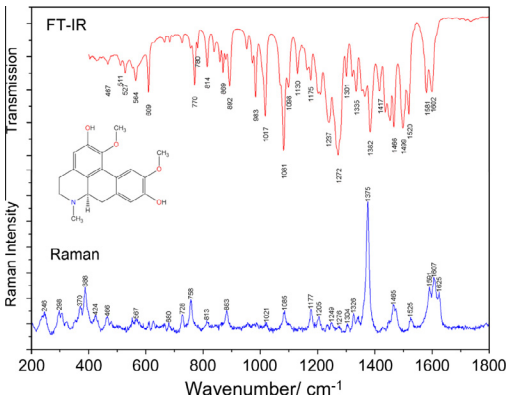

Fig. 6. Infrared and Raman spectra of solid boldine.

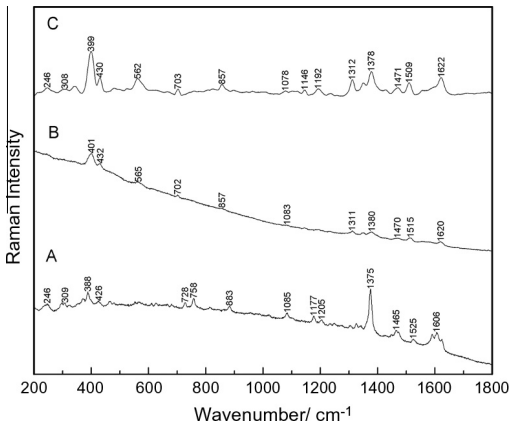

Fig. 8. Raman of boldine crystals (A). SERS 10^{-3} M of the boldine PNps colloidal solution (B). SERS of 10^{-4} M of the boldine PNps colloidal solution dried at room temperature (C).

spectrum of boldine is consistent with a feeble ligand surface interaction. In fact, no new bands or significant wave number shifts of boldine are observed by surface effect which means that no chemical interaction between both components is verified. Intensity changes by surface effect are interpreted on the basis of the SERS selection rules [28] allowing infer about the orientation and organization of the boldine on the Ag surface. By surface effect the strong relative intensity of the CH_3 deformation Raman band at 1375 cm^{-1} decrease; the opposite is observed for the Raman band at 388 cm^{-1} ascribed to a Phe–OH out of plane deformation mode. This spectral behavior is consistent with a methyl group far from the surface and the OH fragment rather close to the Ag substrate. On the other hand, the Raman band at 552 cm^{-1} probably due to a deformation mode of the Phe–O–CH_3 moiety increases its relative intensity, which agrees with a aromatic moiety close to the surface. Others Phe–O–CH_3 Raman bands at 1085 and 1249 cm^{-1} are observed with a similar relative intensity in the SERS spectrum indicating that this moiety is close to the metal surface. The aromatic CC bands, 1500–1600 cm^{-1} spectral region, in the SERS spectrum keep their intensity modes, suggesting that the aromatic rings are not far from the surface. The relative intensity of the SERS band at 1311 cm^{-1} ascribed to the N–CH_3 stretching mode is higher than in the Raman spectrum; this is interpreted in the sense that the vibrating mode has the α_{zz} polarizability component parallel to the incident laser light. Thus, the N–C bond should be perpendicular to the surface. Finally, the out of plane CH modes ascribed to the SERS bands at 702 and 857 cm^{-1} display a relative increasing of their relative intensities by surface effect, which suggests that these vibrations occur perpendicular to the surface. From the above results we propose that some of the two aromatic fragments of the boldine molecule are probably orientated plane parallel to the surface.

For the case of the isolated silver layer, the valence and conduction bands overlap, indicating that the present microscopic model is a good representation of a metallic cluster. EHT results for boldine (confirmed by B3LYP/6-31G and B3LYP/6-311G**++ calculations with full geometry optimization) indicate that the HOMO and LUMO are located mainly on the aromatic rings (that are not exactly coplanar). In the final boldine–Ag geometry (see Fig. 9), the two boldine aromatic rings of boldine, benzo[de] and benzo[g] quinolinic rings, are almost coplanar to the surface. Boldine is located at the center of the Ag layer in which the electronic densities of the HOMO and LUMO (that can be considered respectively as being closer to the upper part of the valence band and the lower part of the conduction band of the cluster) are zero. The aliphatic H-25 and the methoxi H-39, H-40 and H-41 atoms are in the range 2.56–2.9 Å from the cluster. The methoxi O-14 atom is at 2.97 Å and the hydroxyl O-19 atom is at 3.12 Å from the closest Ag atom. The aromatic H-31 and H-37 atoms are at 2.56 and 4.81 Å from the Ag surface, respectively. As the occupied and empty MOs of boldine do not overlap with the HOMO and/or LUMO of the Ag layer a charge transfer is ruled out. Therefore, we may conclude that electrostatic interactions are the main factor of the boldine–Ag layer

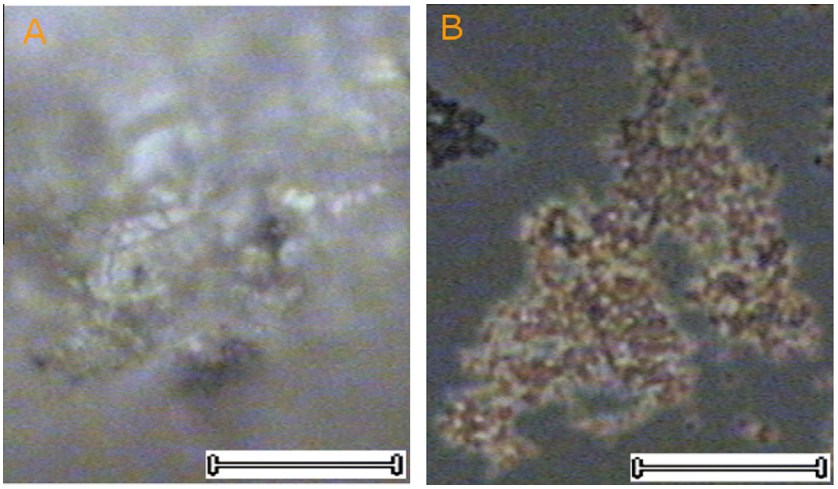

Fig. 7. Boldine crystals (A). 10^{-4} M of the boldine PNps colloidal solution dried at room temperature (B). In the figure is showed a 20 μm line.

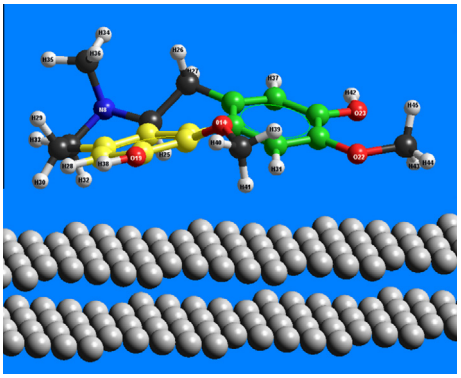

Fig. 9. Molecular model of boldine on an Ag cluster.

interaction. By accepting that the boldine molecule is oriented as in Fig. 9, but on a hot spot and the laser line is perpendicular to the surface, then the N–CH_3 band at 1311 cm^{-1}, the out of plane aromatic CH modes ascribed to the bands at 702 and 857 cm^{-1} and the other out of plane Phe–OH mode at 388 cm^{-1} should be enhanced which is in agreement with the SERS experimental result.

Conclusions

Prismatic silver nanoparticles allow obtaining for the first time the SERS spectrum of boldine with high reproducibility on dry. The SERS spectral analysis supported by selection rules suggests that the boldine molecule exposes the aromatic and heteroatom moieties to the metal surface. An electromagnetic interaction mechanism rather than a chemical one seems to be responsible of the observed spectral enhancement. Molecular mechanics and Extended Hückel Theory for a molecular model of boldine interacting with a silver surface predicts a nearly coplanar orientation of the quinolinic moiety of the analyte on the metal surface, which is in good agreement with the experimental SERS data.

Acknowledgments

We thank Dr. Vicente Castro-Castillo from the Department of Chemistry, Faculty of Sciences, University of Chile, Santiago, Chile, who kindly provided us with the boldine sample. This contribution was financially supported by FONDECYT Chile project 1110106. T.A.A. acknowledges a Doctoral Fellowship from CONICYT. C.G. acknowledges a Doctoral and AT-24121659 Fellowships from CONICYT. R.V. acknowledges a Basal project FB0807-CEDENNA.

References

[1] P. O'Brien, C. Carrasco-Pozo, H. Speisky, Boldine and its antioxidant or health-promoting properties, Chem. Biol. Interact. 159 (2006) 1–17.
[2] A. Valenzuela, S. Nieto, B.K. Cassels, H. Speisky, Inhibitory effect of boldine on fish oil oxidation, J. Am. Oil. Chem. Soc. 68 (1991) 935–937.
[3] M. Baranska, J.Cz. Dobrowolski, A. Kaczor, K. Chruszcz-Lipska, K. Gorz, A. Rygula, J. Raman Spectrosc. 43 (2012) 1065–1073.
[4] N. Misra, S.A. Siddiqui, R. Srivastava, A. Pandey, S. Jain, Spectroscopy 24 (2010) 483–499.
[5] A. Srivastava, P. Tandon, A.P. Ayala, S. Jain, Vib. Spectrosc. 56 (2011) 82–88.
[6] M.V. Cañamares, J.R. Lombardi, M. Leona, J. Raman Spectrosc. 39 (2008) 1907–1914.
[7] Z. Jurasekova, J.V. Garcia-Ramos, C. Domingo, S. Sanchez-Cortes, J. Raman Spectrosc. 37 (2006) 1239–1241.
[8] Z. Jurasekova, C. Domingo, J.V. Garcia-Ramos, S. Sanchez-Cortes, J. Raman Spectrosc. 43 (2012) 1913–1919.
[9] A.J. Frank, N. Cathcart, K.E. Maly, V. Kitaev, J. Chem. Ed. 87 (2010) 1098–1101.
[10] C.I. Cámara, C.A. Bornancini, J.L. Cabrera, M.G. Ortega, L.M. Yudi, Talanta 83 (2010) 623–630.
[11] P. Leyton, J.S. Gómez-Jeria, S. Sanchez-Cortes, C. Domingo, M.M. Campos-Vallette, J. Phys. Chem. B 110 (2006) 6470–6474.
[12] A.E. Aliaga, P. Leyton, I. Osorio-Román, C. Garrido, J. Cárcamo, C. Caniulef, F. Célis, G. Díaz, F.E. Clavijo, J.S. Gómez-Jeria, M.M. Campos-Vallette, J Raman Spectrosc. 40 (2009) 164–169.
[13] A. Aliaga, I. Osorio-Román, C. Garrido, P. Leyton, J. Cárcamo, E. Clavijo, J.S. Gómez-Jeria, G. Diaz F, M.M. Campos Vallette, Vib. Spectrosc. 50 (2009) 131–135.
[14] A.E. Aliaga, H. Ahumada, K. Sepúlveda, J.S. Gómez-Jeria, C. Garrido, B.E. Weiss-López, M.M. Campos-Vallette, J. Phys. Chem. C 115 (2011) 3982–3989.
[15] Hypercube Inc.: 1115 NW 4th Street, Gainesville, FL. 32601, USA.
[16] J.S. Gómez-Jeria, J. Comput. Theor. Nanosci. 6 (2009) 1361–1369.
[17] C. Garrido, A.E. Aliaga, J.S. Gómez-Jeria, J.J. Cárcamo, E. Clavijo, M.M. Campos-Vallette, Vib. Spectrosc. 61 (2012) 94–98.
[18] A.E. Aliaga, T. Aguayo, C. Garrido, E. Clavijo, E. Hevia, J.S. Gómez-Jeria, P. Leyton, M.M. Campos-Vallette, S. Sanchez-Cortes, Biopolymers 95 (2011) 135–143.
[19] P. Leyton, I. Córdova, P.A. Lizama-Vergara, J.S. Gómez-Jeria, A.E. Aliaga, M.M. Campos-Vallette, E. Clavijo, J.V. García-Ramos, S. Sánchez-Cortes, Vib. Spectrosc. 46 (2008) 77–81.
[20] J.J. Cárcamo, A.E. Aliaga, E. Clavijo, C. Garrido, J.S. Gómez-Jeria, M.M. Campos-Vallette, J. Raman Spectrosc. 43 (2012) 750–755.
[21] W. Koch, Int. J. Quant. Chem. 76 (2000) 148–160.
[22] W. Koch, B. Frey, J.F. Sánchez, T. Scior, Z. Naturforsch 58A (2003) 756–784.
[23] M.J. Frisch, G.W. Trucks, H.B. Schlegel et al., Gaussian 03 Rev. E.01, Gaussian Inc., Wallingford CT, USA, 2004.
[24] R. Aroca, Surface-Enhanced Vibrational Spectroscopy, John Wiley & Sons, Chichester, 2006.
[25] Bo-Hong Lee, Ming-Sheng Hsu, Yuan-Chin Hsu, Cheng-Wei Lo, Cheng-Liang Huang, J. Phys. Chem. C 114 (2010) 6222–6227.
[26] D. Lin-Vien, N.B. Colthup, W.G. Fateley, J.G. Graselli, The Handbook of Infrared and Raman Characteristic Frequencies of Organic Molecules, first ed., Academic Press, Boston, 1981.
[27] G. Socrates, Infrared and Raman Characteristic Group Frequencies, Tables and Charts, third ed., JohnWiley & Sons, Chichester, 2001.
[28] M. Moskovits, Rev. Mod. Phys. 57 (1985) 783–826.